Small-Scale Fading for High-Altitude Platform (HAP) Propagation Channels

Fabio Dovis, Roberto Fantini, Marina Mondin, and Patrizia Savi

***Abstract*—In recent years there has been a great interest in the development of high-altitude platforms, which are low cost stratospheric aircraft carrying payloads tailored for a wide range of applications in telecommunications and remote sensing. These platforms are capable of flying at altitudes ranging between 17 and 30 Km, with a potential endurance of weeks to months, features that make them attractive for the provision of future personal communication services. This paper deals with the theoretical derivation of a channel model for the communication link between the platform and terrestrial mobile users or stations. In particular, we address the problem of modeling the small-scale fading effects. It is shown that the particular geometry of the propagation scenario leads to a specific model applicable to the stratospheric channel.**

***Index Terms*—Communication channels, fading channels, multipath channels, radio propagation.**

I. Introduction

THE POSSIBILITY of employing flying platforms in the stratosphere has been recently proposed as a valid alternative to traditional terrestrial or satellite-based infrastructure for the design of future generation communication systems [1]–[4]. Such stratospheric platforms are usually denominated as high-altitude platforms (HAPs) or high-altitude very long endurance (HAVE) vehicles. The term HAPs defines both airships or airplanes, flying at an altitude ranging between 17 and 30 Km in the stratosphere and able to stay aloft for long periods of time (see Fig. 1). The main problem that makes lighter-than-air stratospheric balloons not well suited to telecommunication applications is that it is quite difficult to remotely control their position due to their high sensitivity to weather conditions. Stratospheric airplanes are more reliable and several projects are addressing the design of telecommunication networks based on the use of manned and unmanned aerial vehicles [5]–[8].

The International Telecommunication Union (ITU) has endorsed various frequency ranges for HAPs applications. In particular, the bands 47.2–47.5 GHz and 47.9–48.2 GHz are allocated for fixed services [9]; the frequency range 18–32 GHz is allocated to a number of countries in Region 3 for broadband wireless applications [10]; and the bands 1885–1980 MHz, 2010–2025 MHz, 2110–2170 MHz in Regions 1 and 3, and 1885–1980 MHz and 2110–2160 MHz in Region 2 are allocated to the third-generation wireless communication systems [11].

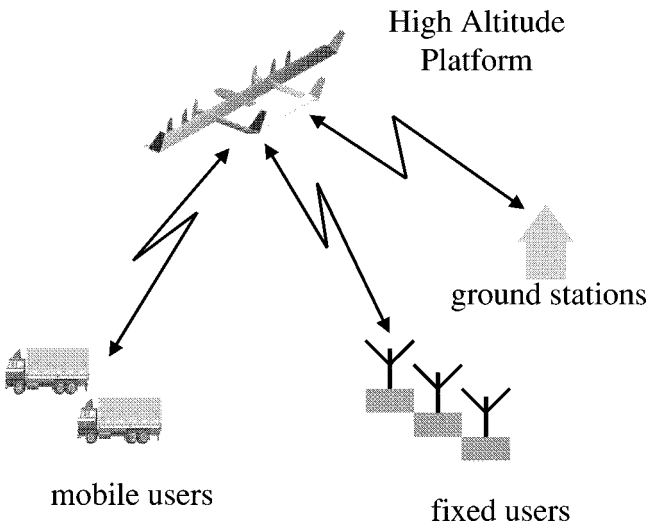

Fig. 1. The system architecture of a HAP communication link.

The most promising telecommunication applications of HAPs are cellular telephony, broadband local multipoint distribution system (LMDS) services, and access provision to digital networks (Internet, ISDN). The flexibility of the system allows for utilization of HAPs not only for carrying telecommunication payloads but also for remote sensing and satellite navigation applications [5], [12].

The major advantages for future services integrating HAPs-based systems are the cost-effective coverage of rural and maritime regions, the system flexibility due to the platforms' mobility on demand (e.g., in emergency situations), and the possibility of upgrading the platform's payload in order to reduce the risk of technology obsolescence experienced with traditional satellites. In addition, HAPs can have a large footprint on earth offering the possibility of providing services over large regions with low expected traffic cost effectively. This is because the use of terrestrial infrastructures would be much more costly due to the underutilization of the large number of transceiver facilities needed to cover the area with low traffic patterns. For example, from an altitude of 17 Km, it is possible to have a coverage region of about 120-Km radius given a minimum grazing angle of 10° [4].

While the research is very active in connection with the aeronautical aspects of HAPs, up to now the telecommunication and propagation aspects of their design have been modeled after terrestrial or satellite systems [13], [14]. Little specific research

Manuscript received March 15, 2001; revised October 1, 2001. This work was presented in part at the International Conference on Elctromagnetics in Advanced Applications (ICEAA) 2001, September 10–14, 2001, Turin, Italy, and in part at the Global Communications Conference (Globecom), November 25–29, 2001, San Antonio, TX (USA).

The authors are with the Dipartimento di Elettronica, Politecnico di Torino, Torino, Italy (e-mail: dovis@polito.it; fantini@mail.tlc.polito.it; mondin@polito.it; savi@polito.it).

Publisher Item Identifier S 0733-8716(02)03384-X.

has been devoted to modeling the stratospheric telecommunication system in order to identify the transmission schemes best suited to such stations [15], [16]. In particular, the available results are mainly focused on atmospheric effects and to the best of our knowledge, no results are available on small-scale fading effects of the channel.

Propagation models have traditionally focused on describing both the average path loss at a given distance from the transmitter (large scale propagation models) as well as the rapid fluctuation of the received power over short distances and/or short time durations (small-scale fading models) (see for example [17], [18]). We define land high-altitude platform channel (LHAP) as the communication link between a terrestrial user (both fixed or mobile) and a HAP.

This paper focuses on the theoretical derivation of the small-scale fading LHAP channel model based on the presence of scatterers on the terrain. In particular, we derive the channel model in the 2-GHz frequency range utilized for cellular and localization applications. Rain attenuation effects are not taken into account since they are negligible at the selected frequency range, while they are predominant at higher frequencies envisaged for some applications of HAPs.

The rest of the paper is organized as follows. In Section II, the small-scale fading characteristics of the LHAP channel are described. The power delay profile is obtained on the basis of a theoretical model derived for terrestrial links by Rappaport and Liberti [19], [20]. This model is extended to the aerial platform-based system. The coherence bandwidth and the coherence time characterizing the LHAP channel are then evaluated. In Section III, theoretical results are used to develop a simulation model of the channel and simulation results are presented in order to highlight its main features. Conclusions are presented in Section IV.

II. Small Scale Fading in a Platform–Based System

Small-scale fading occurs when the received signal, that is the sum of different replicas of the same transmitted signal arriving at the receiver following different paths, experiences constructive and destructive interference over short periods of time and/or short geographical distances due to the relative motion of the transmitter and receiver. As is well known, this causes the received signal level to vary widely over time [21].

From this point of view, a mobile radio channel can be characterized by its power delay profile and its Doppler spectrum [22]. With the growth of cellular and mobile communications, several theoretical and experimental models for the mobile radio channel have been presented (see for example [23]–[25]). Usually these models are developed for ground communication systems with a fixed antenna transmitter. In this section, we analyze the small-scale fading characteristics of an LHAP channel in the case of a transmitter placed on a HAP. First, the power delay profile for a platform-based system is obtained and then the coherence bandwidth and the coherence time are evaluated.

Power delay profiles derived from measurements at ground level are site specific and cannot be adapted to the high-altitude platform case. In order to determine a realistic power delay profile for the platform case, the theoretical model proposed by

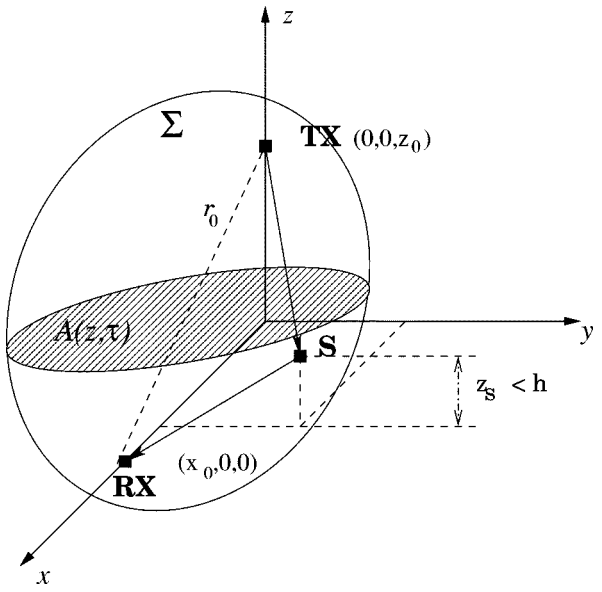

Fig. 2. The ellipsoid Σ is the volume containing all the scatterers that cause excess delays smaller than τ, e.g., scatterer S of height $z_s < h$. The area $A(z, \tau)$ is the intersection of the ellipsoid Σ with an horizontal plane at height z.

Rappaport and Liberti [19], [20] for a ground station (GS) has been considered and extended to the case of a platform station (PS). In this case, the receiver and the transmitter are no longer on the horizontal plane and the height of the transmitter must be taken into account.

Consider the receiver (RX) placed at a point with coordinates (x_0, 0, 0) and the transmitter (TX) at (0, 0, z_0), as shown in Fig. 2. The direct transmission path has length $r_0 = \sqrt{x_0^2 + z_0^2}$ and propagation delay $\tau_0 = r_0/c$, where c is the speed of light. A reflected wave impinging on the receiver with an excess delay τ must have covered a path length given by

$$k(\tau) = r_0 + c\tau.$$

The ellipsoid Σ, with TX and RX as foci, is defined by the set of points whereby the sum of the distance from the transmitter and the distance from the receiver equals $k(\tau)$.

All the scatterers located inside Σ generate a total path length smaller than $k(\tau)$. For this reason, a reflected ray with an excess delay smaller than τ [i.e., a total path length smaller than $k(\tau)$], must be associated with a scatterer S located inside the ellipsoid Σ (see Fig. 2). Since scattered waves are mainly due to tall buildings, trees, poles, or hills that cannot be found above a certain height h, scatterers can be assumed uniformly distributed only in a thin layer close to the ground. As a consequence, the volume $V(\tau)$ containing obstacles that cause a scattered ray with an excess delay smaller than τ is obtained from the intersection between the ellipsoid Σ and the plane $z = h$. Hence, the volume $V(\tau)$ is defined as the set of points (x, y, z) that satisfy

$$\begin{cases} \sqrt{(x-x_0)^2 + y^2 + z^2} + \sqrt{x^2 + y^2 + (z-z_0)^2} < k(\tau) \\ 0 < z < h. \end{cases} \tag{1}$$

The volume $V(\tau)$ can be obtained by evaluating the area $A(z, \tau)$ of the ellipse due to the intersection of the ellipsoid

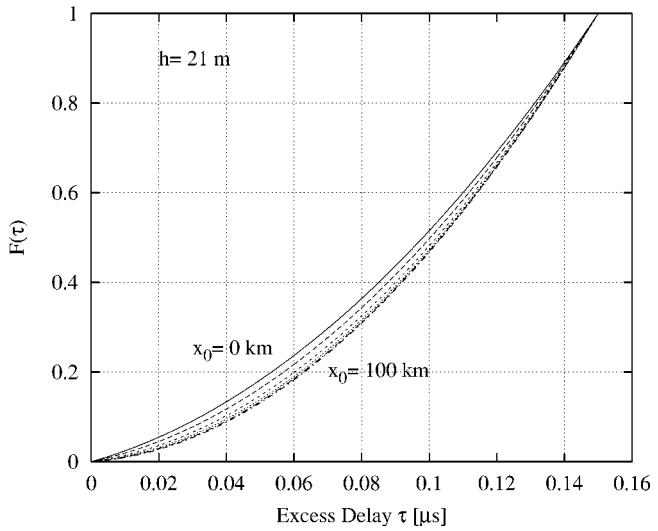

Fig. 3. Excess delay cumulative distribution with $\tau_m = 0.150$ μs, $h = 21$ m, $z_0 = 17$ Km, and x_0 varying from 0 to 100 Km with step 20 Km.

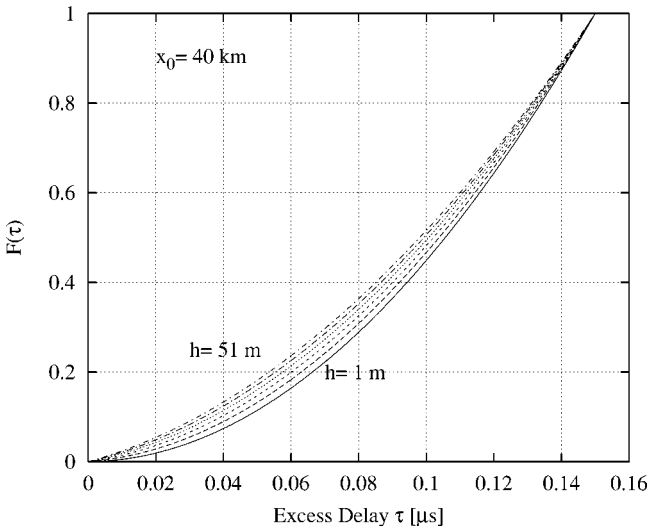

Fig. 4. Excess delay cumulative distribution with $\tau_m = 0.150$ μs, $x_0 = 40$ Km, $z_0 = 17$ Km, and h varying from 1 m to 51 m with step 10 m.

with a horizontal plane of height z (see Fig. 2) and then integrating $A(z, \tau)$ for z varying from 0 to h

$$V(\tau) = \frac{-\pi w(\tau)(r_0 + c\tau)}{4\sqrt{(z_0^2 + w(\tau))^3}} \left[\frac{4}{3}h^3 - 2z_0h^2 - w(\tau)h\right] \quad (2)$$

where $w(\tau) = c^2\tau^2 + 2r_0c\tau$. The cumulative distribution function (cdf) of the excess delay $F_{PS}(\tau)$ can be expressed as the ratio between the volume $V(\tau)$ and the volume that corresponds to the maximum excess delay of the system, $V(\tau_m)$

$$F_{PS}(\tau) = \frac{V(\tau)}{V(\tau_m)} \quad (3)$$

and the probability density function (pdf) can be found by differentiating (3). Equation (3) requires the knowledge of the maximum excess delay τ_m. While values of τ_m for the GS case are well known, there are no measurements available for the platform case. Estimated values of τ_m achieved with conventional aircrafts are in the order of hundreds of nanoseconds, which are much smaller than in the GS case [26].

In Fig. 3 the cumulative distribution function of the excess delay calculated for different values of x_0 and with $\tau_m = 0.150$ μs, $h = 21$ m, $z_0 = 17$ Km are reported; while Fig. 4 shows results calculated for different values of h and with $\tau_m = 0.150$ μs, $x_0 = 40$ Km, $z_0 = 17$ Km. Note that the general shape of the distribution function is the same regardless of the actual values of the parameters used. In practice, the cumulative distribution function of the excess delay is only weakly dependent on the parameters h and x_0. For this reason, in the development of an approximate channel model, a given nominal choice of these parameters, can be used to represent the entire class of cumulative distribution functions.

The knowledge of the cdf of the excess delay allows one to evaluate the average number of echoes $n(\tau)$ having excess delay τ. The power of a single echo having excess delay τ, $P_s(\tau)$ can be evaluated using a free-space model with modified path

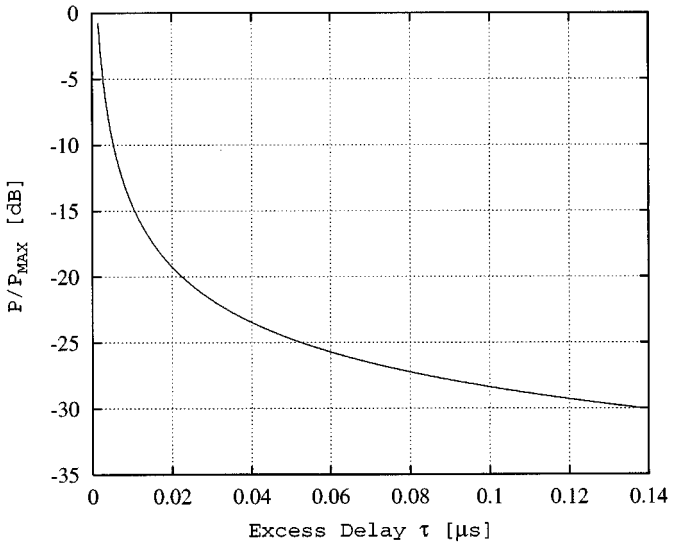

Fig. 5. Normalized power delay profile for a platform-based system.

lengths. The power delay profile of the system can then be obtained as the product of $n(\tau)$ and the power $P_s(\tau)$:

$$P(\tau) = n(\tau)P_s(\tau). \quad (4)$$

Fig. 5 shows the normalized power delay profile obtained for the LHAP channel.

Once the power delay profile of the LHAP channel has been obtained, it is possible to evaluate the *coherence bandwidth* of the channel. As it is shown in [18], this parameter roughly characterizes the channel selectivity when compared to the signal parameters used for communication over the channel. In particular, one can asses whether the channel is selective (i.e., causes Inter-Symbol Interference, ISI) or nonselective for the signal. The coherence bandwidth, defined as the bandwidth over which the frequency correlation is above 0.9, is approximately [24]

$$B_c \approx \frac{1}{50\sigma_\tau} \quad (5)$$

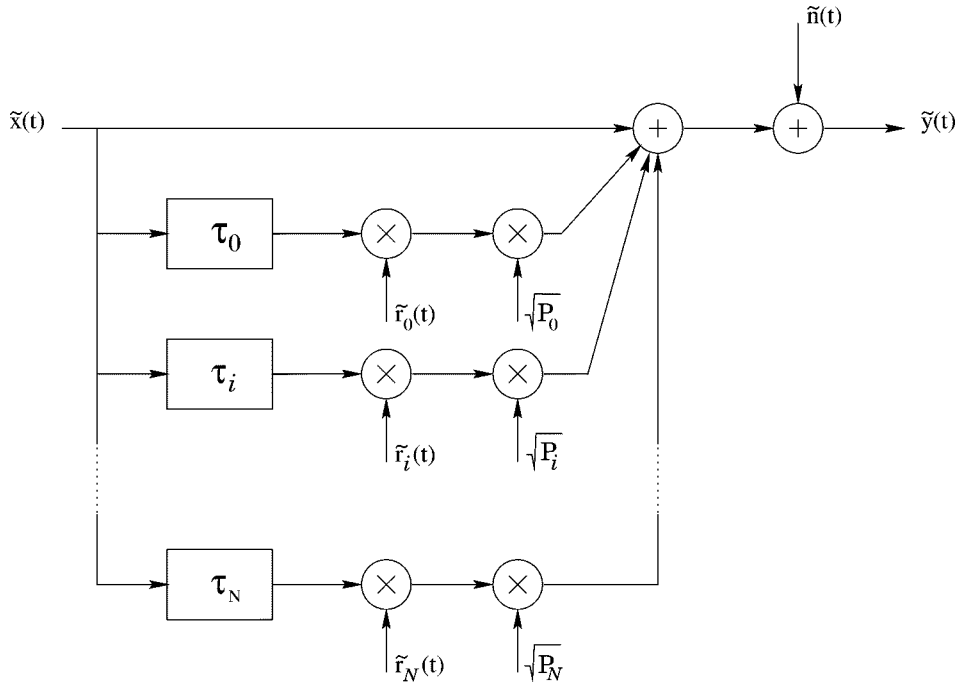

Fig. 6. Diagram of the simulation model used for a fading channel. $\tilde{x}(t)$ is the complex envelope of the input signal, τ_i and P_i are the excess delays and power attenuations given by the power delay profile, $\tilde{r}_i(t)$ are unitary power fading processes, and $\tilde{n}(t)$ represents the white noise process.

and requires the evaluation of the rms delay spread σ_τ that can be obtained from the power delay profile.

The other function characterizing a fading channel, the Doppler spectrum, can be used to determine if the fading is fast or slow. In practice, a simpler parameter, the maximum Doppler spread f_m, can be used which is related to the channel coherence time by the formula [18]:

$$T_c = \frac{9}{16\pi f_m} \tag{6}$$

where the maximum Doppler spread f_m at the carrier frequency f_0 is

$$f_m = f_{d,p} + f_{d,u} = [v_p + v_u]\,\frac{f_0}{c} \tag{7}$$

where v_p is the platform speed and v_u is the user speed [27].

Note that the LHAP channel, having a small delay spread and thus a negligible temporal dispersion, is selective only in the case of wide band signals. On the other hand, the frequency dispersion is more severe if compared with terrestrial channels, because both the movement of the platform and of the mobile receiver contribute to the Doppler spread.

III. Simulation Results

On the basis of the previous analysis, a simulation model of the LHAP channel has been developed with the aim of studying the effects of this channel on the communications between the platform and a mobile terrestrial receiver.

In the simulation model based on the complex envelope representation shown in Fig. 6, the transmitted signal is split into several branches. The upper branch represents the line of sight (LOS) path. Each of the other branches represents a cluster of echoes with mean excess delay τ_i, whereby the time variation effect of the channel is obtained via multiplication by a unity power fading process $\tilde{r}_i(t)$. This fading process has a Gaussian distribution and a bandwidth corresponding to the maximum Doppler spread f_m. Each replica is multiplied by a factor $\sqrt{P_i}$ according to the power delay profile of the channel. Finally, white Gaussian noise $\tilde{n}(t)$ is added to the signal to model all other noises at the receiver.

If the echoes in a given cluster are separated by a delay much smaller than the duration of a transmitted symbol, each branch undergoes a flat (but potentially fast) fading. Dispersion in time is therefore introduced only by the presence of several branches. Different ratios between the power carried by the LOS path (C) and the multipaths (M) can be used depending on the propagation scenario.

The power delay profile has to be discretized in order to obtain a finite number N of delays τ_i and gain factors P_i to use in the simulation model. The sampling interval $\Delta\tau$ must allow a correct representation of the delays τ_i (i.e., it must be equal to or smaller than the minimum separation between two discernable delays).

As an application example, we consider the transmission of a DQPSK modulated signal at a carrier frequency of $f_0 = 2$ GHz. Assuming a platform speed $v_p = 150$ Km/h and a user speed $v_u = 50$ Km/h, the maximum Doppler spread given by (7) is $f_m = 222.16$ Hz leading to a coherence time of $T_c = 0.806$ ms. The power delay profile obtained for the LHAP channel yields an rms delay spread of $\sigma_\tau = 21$ ns. Using (5), a coherence bandwidth of $B_c = 952.38$ kHz is obtained.

In order to verify its usability range, the LHAP channel model has been compared to a more conventional Rician flat-fading model. This model is usually employed whenever transmitter and receiver are in line of sight, as typically assumed in a HAP scenario.

Figs. 7 and 8 depict the sampled scattering diagram of the received signal obtained using the Rician flat fading channel

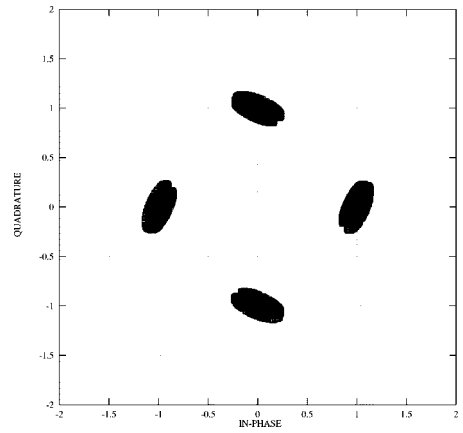

Fig. 7. Scattering diagram of the received signal, obtained for a frequency-flat Rician channel, $C/M = 18$ dB, $Rb = 0.25$ Mb/s.

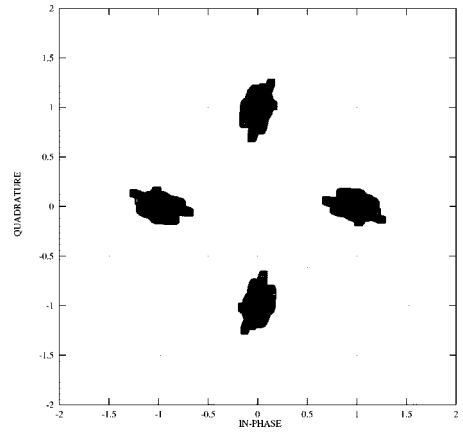

Fig. 8. Scattering diagram of the received signal, obtained for an LHAP channel, $C/M = 18$ dB, $Rb = 0.25$ Mb/s.

model and our model, for a bit rate of 0.25 Mb/s. Both diagrams show a phase shift and a wide spreading of the overall constellation that deteriorate the performance of the transmission system.

Fig. 9 compares the bit-error rate (BER) for AWGN, Rician, and LHAP channel models in the case of $C/M = 18$ dB and bit rate of 0.25, 1, and 4 Mb/s. Note that for a bit rate of 0.25 and 1 Mb/s the LHAP and Rician channel models almost give the same results, while for a bit rate of 4 Mb/s the models behave differently. In particular, the LHAP channel model highlights the performance loss of the modulation scheme which is not correctly described by the Rician model. This bit rate corresponds to a signal bandwidth of about 2 MHz which is greater than the coherence bandwidth of the LHAP channel $B_c = 952.38$ kHz so that the channel becomes selective in frequency and the system performance deteriorates.

The effects of multipath become more evident when the C/M ratio is reduced to 6 dB, as in the case of Fig. 10, where the contribution of multiple echoes highlights the differences among the models. Clearly, in this case the Rician flat fading model is not valid and the more accurate LHAP model has to be used. A significant degradation can be observed when the bandwidth of the transmitted signal exceeds the coherence bandwidth (i.e., for a bit rate of 4 Mb/s), but the effect of the frequency selective channel begins to be visible even at a bit rate of 1 Mb/s.

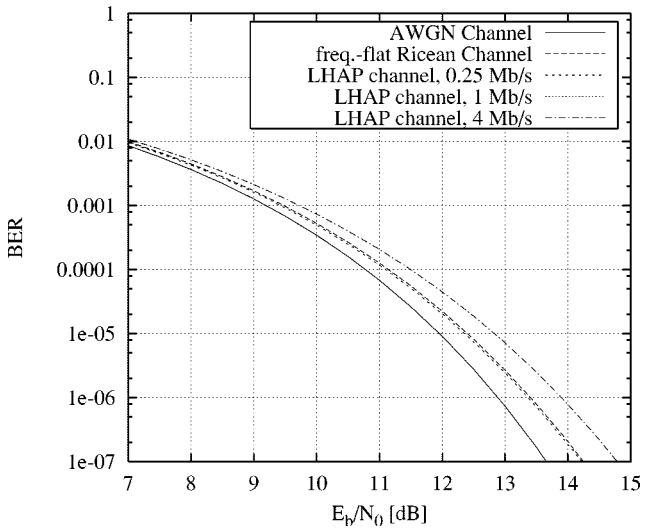

Fig. 9. BER for a DQPSK transmission scheme obtained for AWGN, frequency-flat Rician, and LHAP channel, $C/M = 18$ dB, $Rb = 0.25,\ 1,\ 4$ Mb/s.

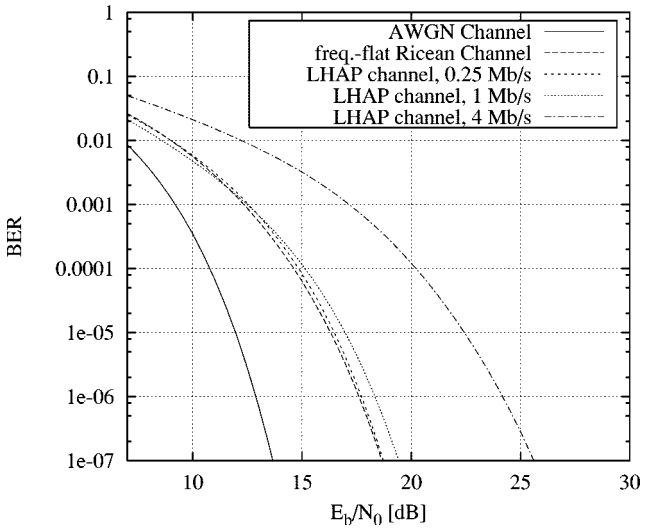

Fig. 10. BER for a DQPSK modulation obtained for AWGN, frequency-flat Rician, and LHAP channel, $C/M = 6$ dB, $Rb = 0.25,\ 1,\ 4$ Mb/s.

TABLE I
ESTIMATED VALUES OF THE SIGNAL-TO-NOISE RATIO NECESSARY TO ACHIEVE A BER OF 10^{-4}, OVER AN AWGN CHANNEL, A FREQUENCY-FLAT RICIAN CHANNEL, AND OVER AN LHAP CHANNEL AT A BIT $Rb = 0.25,\ 14$ Mb/s

E_b/N_0 [dB] BER=10^{-4}	AWGN channel	Rician channel	LHAP channel R_b [Mb/s]		
			0.25	1	4
C/M=18 dB	10.78	11.14	11.09	11.28	11.49
C/M=6 dB	10.78	14.62	14.85	15.14	20.21

In Table I, the values of signal-to-noise ratio (E_b/N_0) necessary to achieve a bit error rate of 10^{-4} are reported. Note that the performance obtained with the Rician frequency flat fading channel model are not dependent on the bit rate because the coherence time $T_c = 0.806$ ms of the channel is always much

greater than the symbol duration (8 μs, 2 μs, and 0.5 μs for a bit rate of 0.25, 1, and 4 Mb/s, respectively). It has to be pointed out that in order to observe the complete behavior of the fading process, the system has been simulated for a time longer than the coherence time T_c of the LHAP channel.

IV. Conclusion

In this paper, the theoretical derivation of a channel model for the communication link between HAPs and terrestrial users or ground stations is presented. In particular, small-scale fading effects are considered and the model by Rappaport and Liberti is extended to the LHAP channel scenario. The power delay profile is derived and the coherence bandwidth and the coherence time of the LHAP channel are evaluated. Simulation results show the dispersive effects of the LHAP channel and demonstrate that channel models that do not consider the presence of scatterers close to the ground (i.e., Rician flat fading channel) can yield to overly optimistic results.

Acknowledgment

The authors would like to thank the reviewers for their comments that helped to improve the quality of this paper and Prof. F. Daneshgaran, California State University, Los Angeles, for his valuable suggestions and help.

References

[1] G. M. Djuknic, J. Freidenfelds, and Y. Okunev, "Estabilishing wireless communications services via high altitude platforms: A concept whose time has come?," *IEEE Commun. Mag.*, pp. 128–135, Sept. 1997.

[2] C. A. Robinson, Jr., "High capacity aerial vehicles aid wireless communications," *Signal*, pp. 16–20, Apr. 1997.

[3] D. Grace, N. E. Daly, T. C. Tozer, and A. G. Burr, "LMDS from high altitude aeronautical platforms," in *IEEE GLOBECOM'99*, Rio de Janeiro, Brazil, Dec. 1999, pp. 2625–2629.

[4] F. Dovis, M. Mondin, and P. Mulassano, "On the use of HALE platforms as GSM base-stations," *IEEE Pers. Commun. Mag.*, pp. 37–44, Apr. 2001.

[5] HeliNet project website. Politecnico di Torino, Turin, Italy. [Online]. Available: http://www.helinet.polito.it

[6] Global Hawk website. Northrop Grumman, Los Angeles, CA. [Online]. Available: http://www.northgrup.com

[7] HALOstar Network. Angel Technologies Corporation, Washington, DC. [Online]. Available: http:/www.angeltechnologies.com

[8] Sky Station International, Washington, DC. [Online]. Available: http://www.skystation.com

[9] "Preferred characteristics of systems in the fixd service using high altitude platforms operating in the bands 47.2–47.5 GHz and 47.9–49.2 GHz," International Telecommunication Union, Geneva, Switzerland, ITU-R Resolution 122, 1997.

[10] "Technical and operational characteristics for the fixed service using high altitude platform stations in the frequency range 18–32 GHz," International Telecommunication Union, Geneva, Switzerland, ITU-R f.[9B/Ka–HAPS], 2000.

[11] "Minimum performance characteristics and operational conditions for high altitude platform stations providing IMT-2000 in the bands 1885–1980 MHz, 2010–2025 MHz and 2110–2170 MHz in region 1 and 3 and 1885–1980 MHz and 2110–2160 MHz in region 2," International Telecommunication Union, Geneva, Switzerland, ITU-R Recommendation F.1456,, 2000.

[12] Environmental Research Aircraft and Sensor Technology. National Aeronautica and Space Administration, Washington, DC. [Online]. Available: http://www.dfrc.nasa.gov/Projects/Erast/index.html

[13] E. Lutz, D. Cygan, M. Dippold, F. Dolainsky, and W. Papke, "The land mobile satellite communication channel-recording, statistics and channel model," *IEEE Trans. Veh. Technol.*, vol. 40, pp. 375–386, May 1991.

[14] R. M. Barts and W. Stutzman, "Modeling and simulation of mobile satellite propagation," *IEEE Trans. Antennas Propagat.*, vol. 40, pp. 375–382, Apr. 1992.

[15] C. Oestges and D. Vanhoenacker-Janvier, "Coverage modeling of high-altitude platforms communication systems," *Electron. Lett.*, vol. 37, no. 2, pp. 119–121, Jan. 18, 2001.

[16] J.-M. Park, B-J Ku, and D.-S. Ahn, "The simulation modeling and performance analysis of stratospheric communications system," in *Proc. 4th Int. Symp. Wireless Personal Multimedia Communications*, Aalborg, Denmark, Sept. 9–12, 2001, pp. 1641–1644.

[17] H. L. Bertoni, *Radio Propagation for Modern Wireless Systems*. Englewood Cliffs, NJ: Prentice-Hall, 2000.

[18] T. S. Rappaport, *Wireless Communications: Principles and Practice*. Englewood Cliffs, NJ: Prentice-Hall, 1996.

[19] T. S. Rappaport and J. C. Liberti, "A geometrically based model for line-of-sight multipath radio channels," in *Proc. 46th IEEE Vehicular Technology Conf.*, Atlanta, GA, Apr./May 1996, pp. 844–848.

[20] ——, *Smart Antennas For Wireless Communications: IS-95 and Third Generation CDMA Applications*. Englewood Cliffs, NJ: Prentice Hall, 1999.

[21] W. C. Jakes, *Microwave Mobile Communications*. Piscataway, NJ: IEEE, 1994.

[22] J. D. Parson and J. G. Gardiner, *Mobile Communication Systems*. Glasgow, U.K.: Blackie and Son, 1989.

[23] A. G. Burr, "Wide-band channel modeling using a spatial model," in *IEEE 5th Int. Symp. Spread Spectrum Techniques and Applications*, vol. 1, 1998.

[24] W. C. Y. Lee, *Mobile Cellular Telecommunications System*. New York: McGraw Hill, 1989.

[25] V. Erceg et alii, "A model for the multipath delay profile of fixed wireless channels," *IEEE J. Select. Areas Commun.*, vol. 17, Mar. 1999.

[26] M. Döttling, A. Jahn, J. Kunisch, and S. Buonomo, "A versatile propagation channel simulator for land mobile satellite applications," in *Proc. 48th IEEE Vehicular Technology Conf.*, May 1998, pp. 213–217.

[27] M. Pent *et al.*, "HELIPLAT as a GSM base station: The channel model," in *6th Int. Workshop Digital Signal Processing Techniques for Space Applications DSP '98* Noordwijk, The Netherlands, Sept. 23–25, 1998.

Fabio Dovis was born in Bruino (TO), Italy, in 1970. He received the degree in electronics engineering, in 1996, and the Ph.D. degree in electronics and communications engineering in February 2000, both at Politecnico di Torino.

Since 2000, he has been with the Electronics Department of Politecnico di Torino where he is currently an Assistant Professor. In 1998 he was a Visiting Researcher at the California State University, Los Angeles. His research interests include the application of wavelet waveforms to telecommunications for the design of multicarrier systems. He is member of a team addressing the design of personal communication systems based on high altitude platforms (HAPs). Other topics of interest are navigation and positioning based on global navigation satellite systems and cellular networks, and the design of HAP-based augmentation systems for GPS and Galileo.

Roberto Fantini was born in Biella, Italy, on September 16, 1976. He received the "Laurea" degree (*summa cum laude*) in telecommunications engineering from Politecnico di Torino, Turin, Italy, in 2001.

He is presently with the Dipartimento di Elettronica, Politecnico di Torino. His current research interests include RF propagation and wireless communication. He is particularly interested in characterising radio wave propagation and in developing simulation models for high altitude stratospheric platforms. He is currently collaborating with the Centre for Multimedia Radio Communications (CERCOM) of Politecnico di Torino and with the HeliNet team which is developing.at Politecnico di Torino a network of stratospheric platforms for the provision telecommunication services.

Patrizia Savi received the "Laurea" degree in electronic engineering from the Politecnico di Torino, Turin, Italy, in 1985.

In 1986, she worked on the analysis and design of dielectric radomes at Alenia (Caselle Torinese). Since 1987, she has been a reasercher of Centro Studi Propagazione e Antenne of the Italian National Research Council (CNR) at Politecnico di Torino. Since 1998, she has been a member of the Department of Electronics at Politecnico di Torino as an Associate Professor. She teaches courses on electromagnetic field theory. Her research interests include the areas of dielectric radomes, frequency selective surfaces, waveguide discontinuities and microwave filters, and finite elements method. Her current research deals with wireless radio channel modeling.

Marina Mondin was born in Turin, Italy. She received the Laurea degree in electronics engineering (*summa cum laude*), in 1986, and the Ph.D. degree in electronics engineering, in 1990, both from Politecnico di Torino, Turin, Italy

In 1987, she was recepient of the "De Castro" scholarship, and she spent the year 1987–1988 as Vising Scholar in the Department of Electrical Engineering at the University of California, Los Angeles. Since 1990, she has been with the Electronics Department of Politecnico di Torino, where she is currently an Associate Professor. Her current interests are in the areas of turbo coding, simulation of communication systems, digital communications, and software radio.

Dr. Mondin is a member of the IEEE Communications an Information Theory Societies.